LARS Contract Report 061579

# Reconstruction of Geophysical Surfaces from Track-Type Surveys

by **Paul E. Anuta**
**Clare D. McGillem**

Prepared for
**The National Science Foundation**
Engineering Division
Washington, D. C.
Program Director: **Dr. Norman Caplan**

Grant No. ENG-7614400

Submitted by
**Laboratory for Applications of Remote Sensing**
**Purdue University**
**West Lafayette, Indiana 47907**

# RECONSTRUCTION OF GEOPHYSICAL SURFACES FROM TRACK-TYPE SURVEYS

by

P. E. Anuta
C. D. McGillem

## ABSTRACT

The problem of reconstruction of a continuous or densely sampled uniform grid scalar surface from track-type geophysical surveys is discussed. The signal sources considered include earth gamma ray radiation and magnetic fields measured at low altitude (typically 500 ft.) along tracks spaced from a fraction to several miles apart. The signal model investigated assumes the geophysical surface consists of a narrow band isotropic stochastic signal process. The sampling process is characterized by a high sampling rate along track and a low sampling rate across track. A reconstruction filter approach is described which attempts to provide isotropic reconstruction to minimize the error in representation of scene features.

---

This work was sponsored by the National Science Foundation under Grant ENG-7614400.

# I. INTRODUCTION

Many geophysical remote sensing surveys utilize non-imaging sensors carried in low flying aircraft along parallel tracks over a survey site. The survey produced by these sensors is sampled at a high rate relative to the field of view producing nominally an oversampled sequence. However, due to intuitive judgements regarding the size of features and economic limitations the spacing between tracks is many times the along track sampling interval. Figure 1 shows an example of the sampling structure which results. Typical sensors are gamma ray radiometers, earth field magnitometers, gravity sensors, induced magnetism sensors, atmospheric aerosal detectors and others.

It is desirable to carry out analysis of track type survey data in image format to utilize the knowledge and techniques of visual image interpretation. Contouring is also widely used to display the data in two dimensional format. Registration of track type data with a densely sampled image such as from Landsat scanners is often required. In order to implement these image analysis procedures a uniform closely spaced grid of points is required. The filtering and interpolation method used to generate the grid of points from the original data must reconstruct shapes and features as they would have appeared in a uniformly sampled case. Should anisotropic reconstruction occur shapes and lineations in images or contour plots could be distorted and result

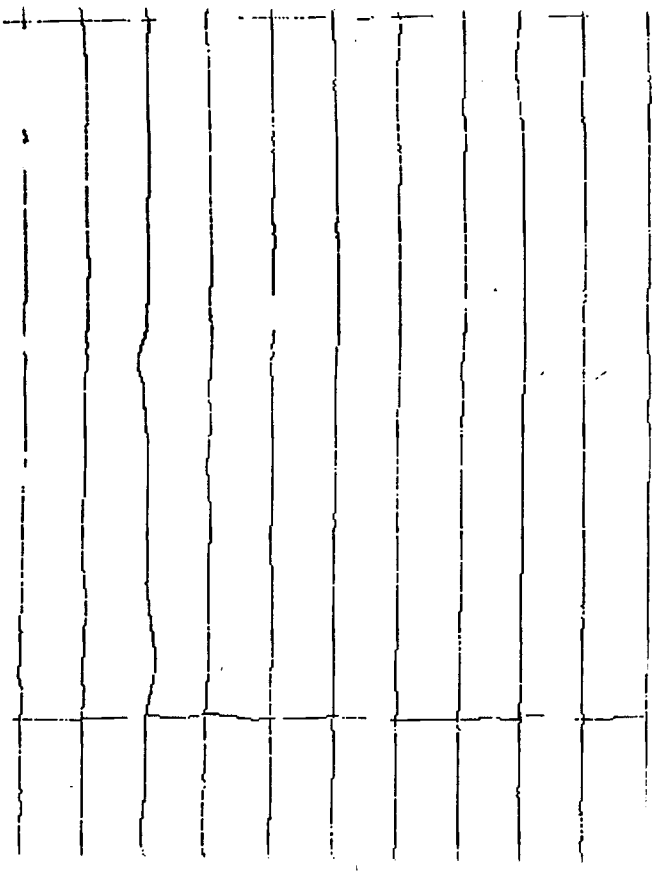

Figure 1. Example of Track-Type Survey Data Locations. Southeast Arizona Site.

in misleading interpretation with resultant waste of prospecting investment (1).

Figures 2 and 3 show image reconstructions of uranium gamma ray survey data from a site in southeast Arizona (2). The along track samples are spaced at about 450 ft. and the tracks are spaced nominally 3 miles apart. Figure 2 was created from a 500 ft. square grid obtained by interpolation across the tracks with about 30 new samples generated between each track. Note the striped and extremely distorted appearance of the image. Figure 3 is an image generated by low pass filtering the along track sequence and then across track interpolating using a cubic spline. Note the change in shape in the image in the different reconstructions. Clearly an isotropic filtering and interpolation method is needed to insure good image generation under conditions of arbitrary along the across track sampling regimes. This report presents results of research on an approach to reconstruction of a uniform grid from a track-type survey.

## II. DATA SET DESCRIPTION AND ASSUMPTIONS

The track-type survey used as an example in this study was flown by Texas Instruments Co. Exploration Services Group for the U. S. Dept. of Energy (2). The aircraft operated at a nominal altitude of 400 ft. above terrain and collected gamma ray radiation for three elements (uranium, thorium, potassium) and also earth magnetic field data. The along track sample interval was nominally 450 ft. and nominal track spacing was 3 miles. Only the uranium data was considered in this study. A graph of a segment of one flight line is shown in Figure 4.

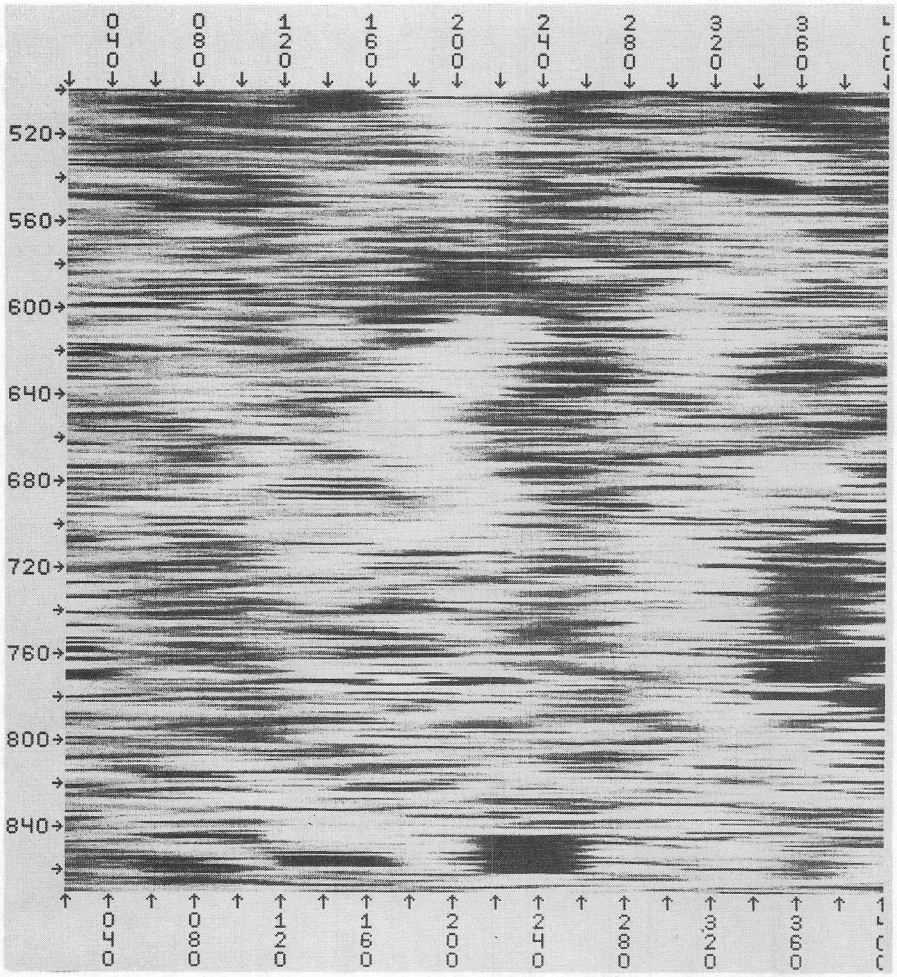


Figure 2. Image Reconstruction of Track-Type Data Using Across Track Interpolation With No Along Track Filter.

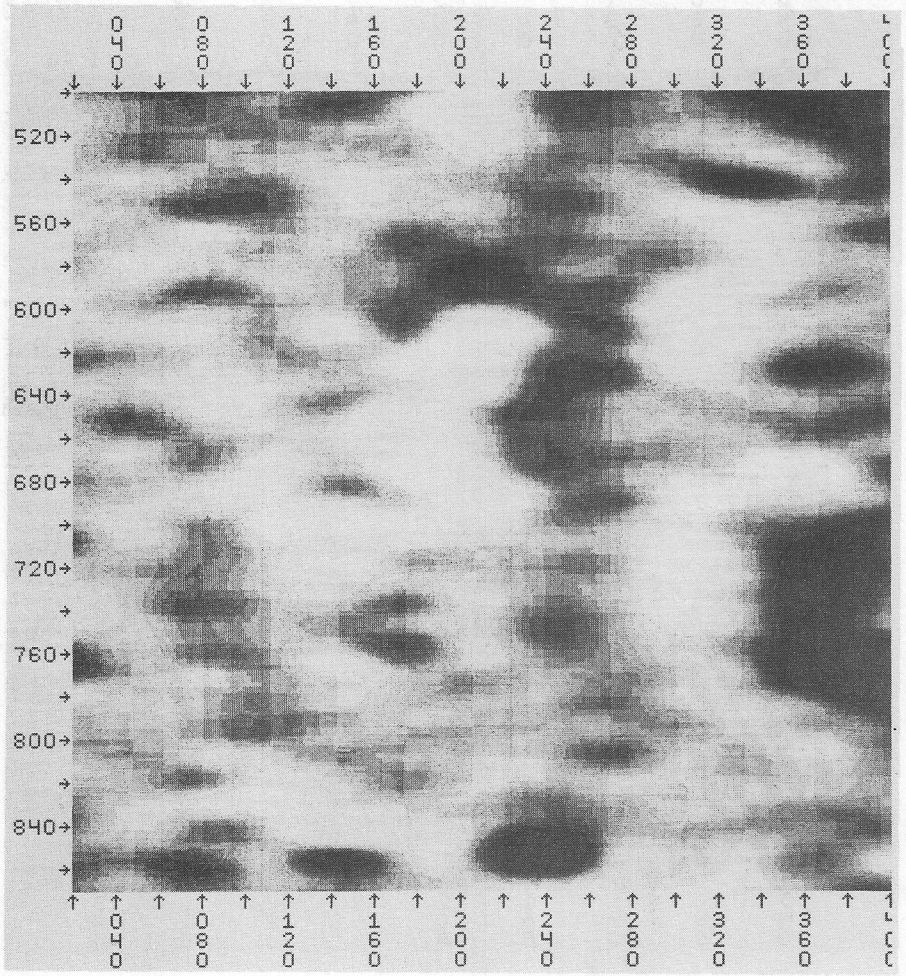


Figure 3. Reconstruction as in Figure 2 but with Low Pass Along Track Filtering.

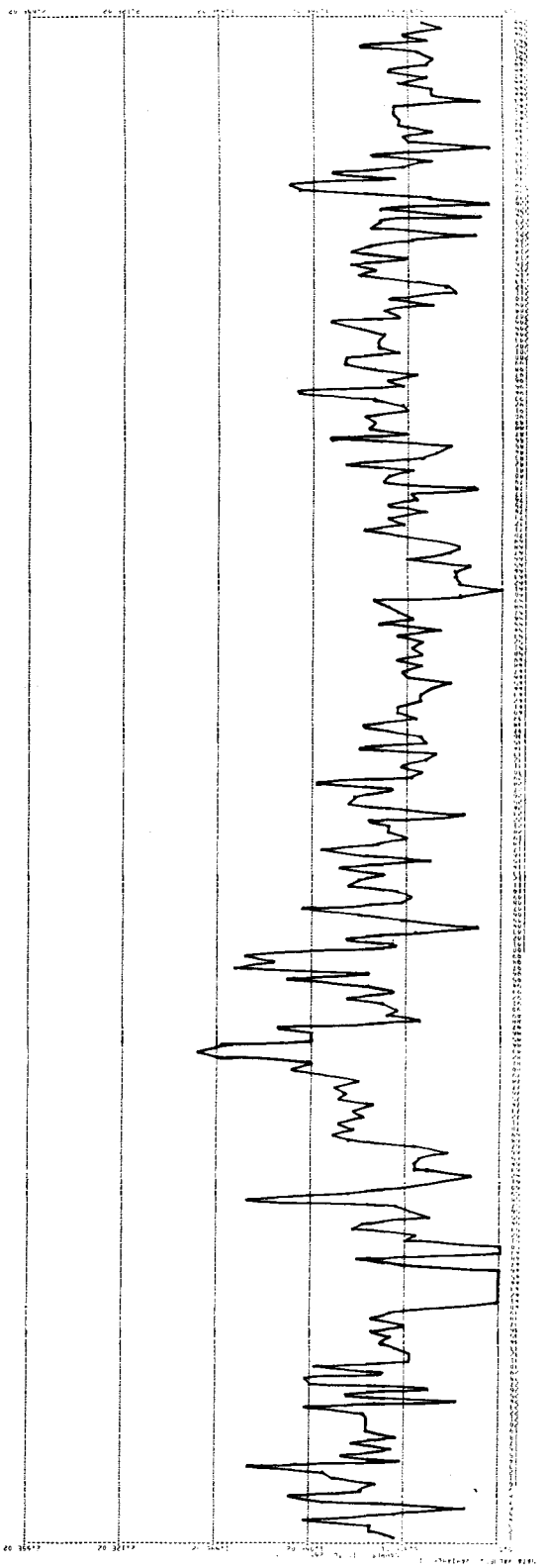

Figure 4. Example of Gamma Ray Radiation Data from Southeast Arizona Site. Plot Covers Approximately 22 Miles.

The data structure assumed for the study is a two dimensional planar orthogonal coordinate system with the X axis vertical increasing downward on a graph with the X direction being the along track direction. The Y axis is the across track direction and positive is to the right or "east." The frequency variables are in units of cycles per unit distance, e.g., cycles/ft., and u is along track frequency and v is across track frequency. The along and across track sample spacing is assumed constant with the along track interval denoted by d and the track spacing by D.

The signal model assumption made for the current study is that the geophysical scene is an isotropic random surface with a negative exponential autocorrelation function. This enables tractable analysis and the model is considered to be a reasonable representation of the actual scene. The a.c.f. is then separable and of the form:

$$\phi(\tau,\mu) = e^{-a_x|\tau|}\, e^{-a_y|\mu|}$$

where: $\tau$ and $\mu$ are x and y direction lags

$a_x$ and $a_y$ are correlation parameters and since an isotropic scene is assumed $a_x=a_y=a$.

## III. ISOTROPIC INTERPOLATION CRITERION

The requirement for isotropic interpolation of the track survey comes about due to interest in multivariate digital analysis of a number of remote sensing and ancillary data types. The problem addressed here is the reconstruction of track-type

survey data to a uniform grid so that it can be registered with other variables at a small grid size relative to the track spacing. The requirement for the grid size to be smaller than the track spacing comes about from the desire to save as much of the resolution as possible of sensors such as Landsat. For the example in this study the Landsat has a nominal resolution of 250 ft. and the gammaray data has a track spacing of 3 miles. A reference grid size of 500 ft. was chosen as a reasonable compromise to maintain the image quality of Landsat and the resolution inherent in the geology map data merged with the remote sensing data. Thus, nominally 30 samples need to be generated between each track of the gamma ray data.

The isotropic reconstruction requirement then becomes one of matching the frequency response characteristics of an along track filter to an across track interpolator to produce a result that does not distort shapes and structures in the geophysical "scene." Several error criterion are candidates; however, the Tchebyshef or maximum error measure is most widely accepted for controlling and frequency characteristics of filters (3). The basic requirement is thus to design an across track interpolator with frequency response $H_y(v)$ and an along track filter with frequency response $H_x(u)$ such that:

$$e_I = \max_v |H_x(v) - H_y(v)| \qquad o \leq v \leq 1/2D$$

is a minimum. V is the spatial frequency variable and the maximum frequency of interest is 1/2D where D is the across track

spacing. The scene process will generally have wider bandwidth than this and aliasing will be present due to the undersampling resulting from the track spacing D.

The second consideration is to control the amount of aliasing in the across track interpolated signal. To accomplish this we define the signal-to-alias noise ratio (SANR) as the ratio of the power in the baseband at a particular frequency to all the alias power at other frequencies. Since we are assuming a separable process:

$$S_{xy}(u,v) = S_x(u)\ S_y(v)$$

The spectrum of the sampled signal in the across track dimension is:

$$S_y(v) = \frac{1}{D} \sum_{k=-\infty}^{\infty} S_y(v-k/D)$$

The ratio of the power in the base band to the total alias power from all other images of the spectrum is the SANR:

$$SANR(V) = \frac{S_y(v)}{\frac{1}{D} \sum_{h=-\infty}^{\infty} S_y(v-k/D)} \quad k \neq 0 \qquad \frac{-1}{2D} \leq v \leq \frac{1}{2D}$$

The power spectral density for the exponential a.c.f. $\phi_y(\tau) = e^{-a|\tau|}$ is:

$$S_y(v) = \frac{2a}{a^2 + 4\pi^2 v^2}$$

The SANR is plotted in Figure 5 for values of a from .1 x $2\pi$ to .5 x $2\pi$ and for values of v from 0 to .5 assuming D-1. A threshold level can be chosen from this plot to keep the ASNR above the threshold up to the threshold frequency. Implementing a low pass filter cutting off at the threshold frequency will then eliminate frequencies having SANR values below the threshold.

In the work reported here only the isotropy constraint was used. Methods using alias control are being studied but no results were available for this report.

## IV. POLYNOMIAL INTERPOLATOR CHARACTERISTICS

A large number of polynomial interpolation methods exist and choosing one for a particular application depends on many factors. Low degree interpolators are simple to implement and have a long history of use. We are concerned here with frequency response characteristics and it becomes difficult to determine these characteristics for high degree cases. Digital filter theory is usually used to analyze high degree cases. For the case at hand efficiency is of the greatest interest since a large number of points are to be generated between each track. In addition to low degree polynomials, spline interpolators using polynomials possess some attractive characteristics and are of interest in this study (4). The frequency characteristic of interest is the power transfer function which is the magnitude squared of the Fourier transform of the interpolating pulse for

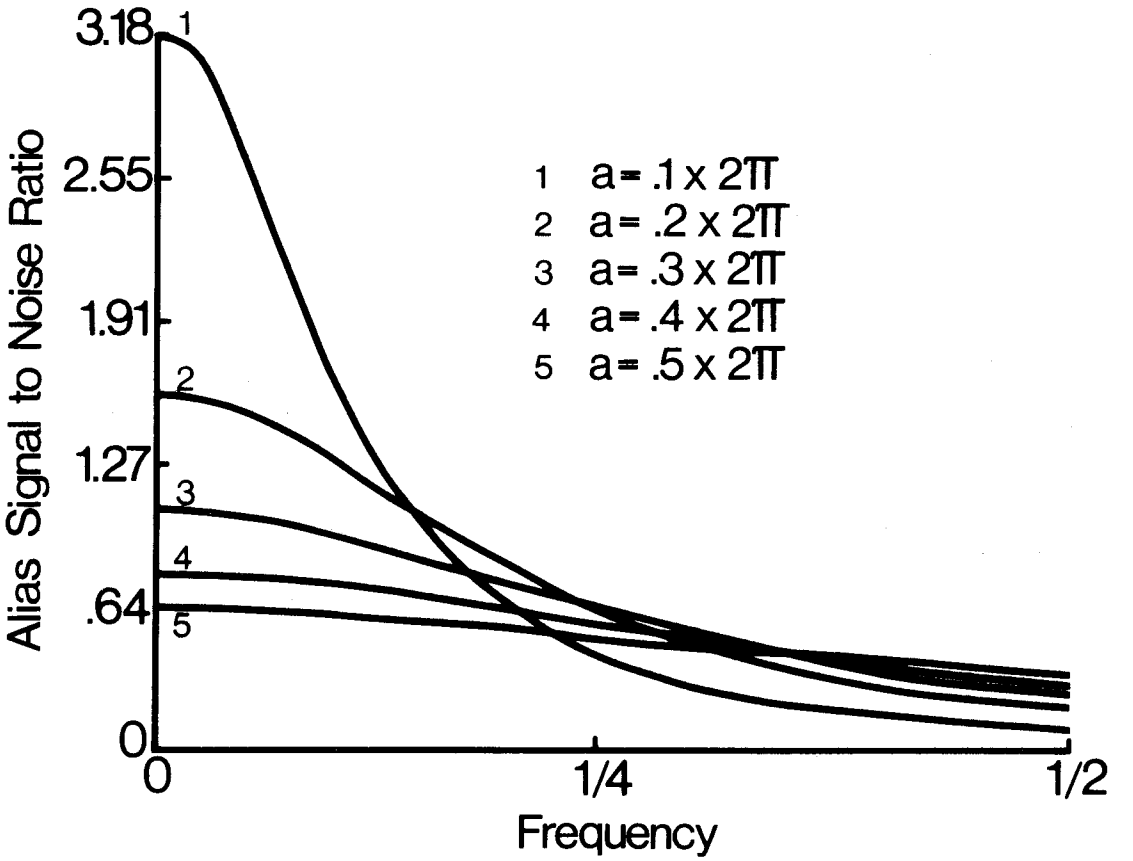


Figure 5. Signal to Alias Noise Ratio for Values of Parameter a from .1 x 2π to .5 x 2π.

polynomial interpolators. For spline interpolators it is more complex (See Appendix). Five cases will be discussed first, third and fifth degree polynomials and third and fifth degree spline interpolators.

The simplest approach to interpolation is the linear case in which a straight line is passed through each pair of original samples. We assume initially that a continuous interpolated signal is being generated. The general input output relationship is:

$$g(x) = \sum_{k=-\infty}^{\infty} f(kD)\ h(x-kD)$$

where: f is the input, g is the output
h is the interpolating pulse
D is the sample interval

The h(x) for linear interpolation is a triangular pulse of width 2D and the power transfer function is:

$$|H_1(u)|^2 = \left(\frac{\sin \pi uD}{\pi uD}\right)^4$$

Similarly the cubic and fifth order cases can be evaluated from the Fourier transforms of their interpolating pulses (5). The analytical expressions for the higher degree cases are quite complex and direct transformation is used to evaluate these

cases. The details of generating the transfer functions are presented in the Appendix.

The first degree spline is the same as linear interpolation and has the same response as given above. Cubic and fifth degree splines fit a polynomial between each data pair and maintain continuity of Q-1 derivatives for a Q degree spline. Note that even order cases are not discussed due to the nonlinear phase characteristics of both polynomial and spline interpolators of even order. It can be shown that the power transfer characteristics of the cubic and fifth degree splines are (6):

$$|H_3(u)|^2 = \left(\frac{3}{(2 + \cos 2DuD)}\right)^2 \left(\frac{\sin \pi uD}{\pi uD}\right)^8$$

$$|H_5(u)|^2 = \frac{(120)^2}{(2\pi uD)^8} \left(\frac{6 - 8\cos 2\pi uD + 2\cos 4\pi uD}{66 + 52\cos 2\pi uD + 2\cos 4\pi uD}\right)^2 \cdot \left(\frac{\sin \pi uD}{\pi uD}\right)^4$$

The linear frequency response characteristics for these five polynomial based interpolators are plotted in Figure 6 for frequencies from 0 to 2/D or four times the Nyquist frequency of the sampled sequence. The responses of the increasing degree polynomial cases improve with increasing degree as expected; however, note that the cubic spline has significantly better response than the cubic polynomial and the same is true for the fifth degree spline versus the fifth degree polynomial. It is

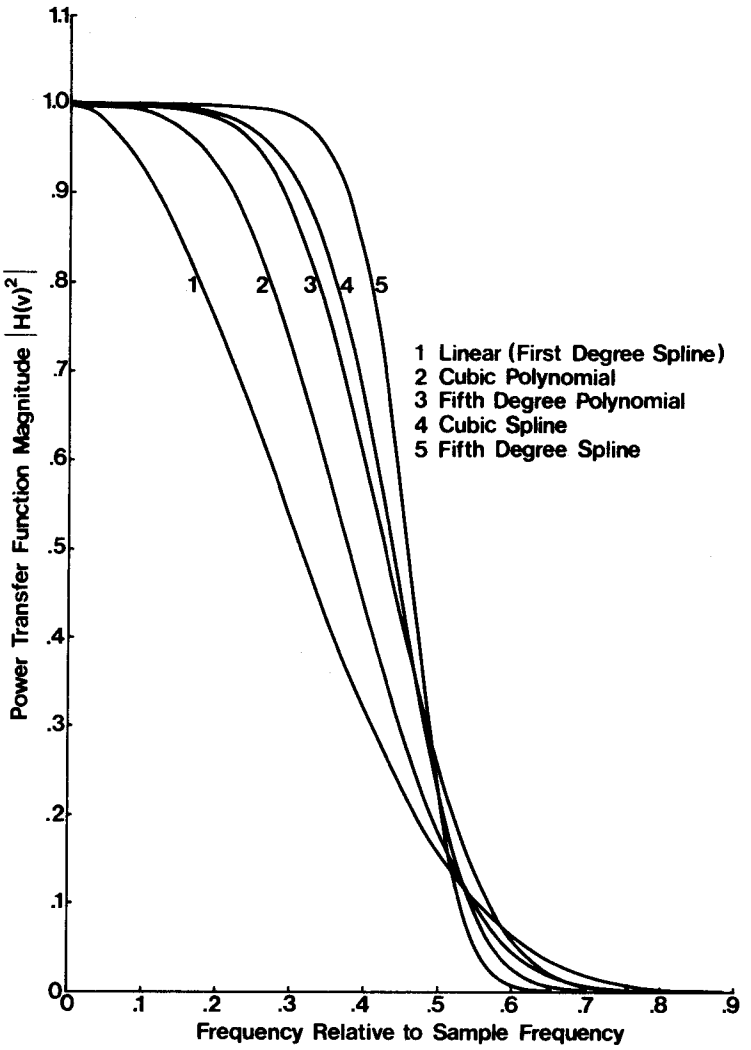


Figure 6. Power Transfer Functions for Polynomial and Spline Interpolation Methods.

also of interest to note that even if the sampled sequence is bandlimited to 1/2D the continuous output signal has spatial frequencies above 1/2D which can be considered aliases and if the interpolated continuous signal is resampled at D there will be aliasing in the resampled signal due to folding of the response of H(v) from 1/2D to infinity. Also note that the performance of the cubic spline is obtained at the cost of three multiplies per new sample point plus spline generation overhead whereas the poorer performance of the cubic interpolator costs four multiplies per new point but with no overhead (if a table lookup approach is used for the polynomial coefficients.) This relationship will be explored in more detail below.

## V. DIGITAL FILTER INTERPOLATORS

Windowed sinc function or optimum FIR filters can be used to generate interpolation pulses which perform the same function as the classical polynomial interpolators and are easier to design for degrees higher than five. An FIR filter with bandpass of 1/2D will result in essentially the same interpolating pulse as the polynomial for the same degree. A sinc function filter having a cutoff frequency $f_c$ and utilizing a Hanning window has the form:

$$h(x) = 2f_c \left\{ \frac{\sin 2\pi f_c x}{2\pi f_c x} \right\} (.5 + .5 \cos \pi x/\tau)$$

where: $f_c$ is the cutoff frequency

$x$ is the continuous space variable

$\tau$ is the width of the window

The Fourier transform of this filter function can be expressed as a convolution (7):

$$H_s(v) = \int_{-f_c}^{f_c} \frac{\sin 2\pi ND(v-\xi)}{2\pi ND(v-\xi)} \quad \frac{d\xi}{1-(2ND(v-\xi))^2}$$

This frequency response magnitude squared is plotted in Figure 7 for $f_c$=1/2D and N=2. This case corresponds to the cubic polynomial case and is the result for a filter of length 5 which for interpolation would require four multiplies per new point. Also plotted is the response for the cubic polynomial and cubic spline. Note that the cubic spline has significantly better response up to the Nyquist frequency than the cubic polynomial or sinc based filter.

The evidence generated for these low order interpolators indicated that for methods using three to four multiplies per new point the cubic spline may be an attractive approach and was used in the system to be discussed.

## VI. AN APPROACH TO ISOTROPIC RECONSTRUCTION

A number of considerations must be made when designing a processor for transforming a track survey into a uniform grid not the least of which is cost. In real survey there are many points along the tracks which do not have data due to equipment problems and terrain or flight path factors. Often data is present but the tracks deviate due to aircraft avoid once maneuvers mountains due to and other obstacles.

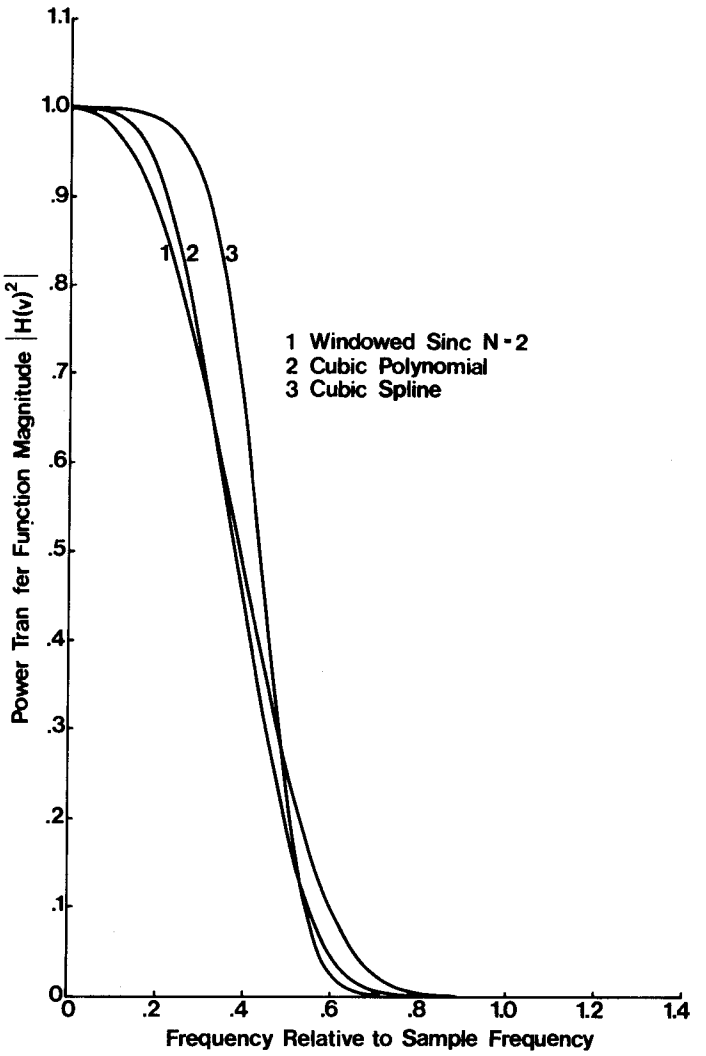


Figure 7. Comparison of Transfer Functions for Cubic, Cubic Spline and Sinc, N=2, Interpolators.

An approach was taken in the case in question in this study in which a cubic spline was used for the across track interpolator. This method gives better signal performance than linear, cubic polynomial or four point sinc filter at a cost of only three multiplies per new point plus boundary condition overhead. Also, since the number of tracks in a survey is generally very small compared to the number of samples along the tracks the spline can easily be set up to use all the points across the survey and avoid the end effects of a non-causal FIR filter approach. In the survey used in this study there were 52 tracks with 1650 samples along each track. The spline also allows arbitrary spacing between tracks and of course the derivatives at the points are continuous up to second.

The along track filtering problem then becomes one of matching the frequency characteristics to that of the across track scheme. The use of splines is not advisable due to the discontinuous nature of the data and large data extent. An FIR filter was chosen since the frequency characteristics could be easily matched to that of the across track spline. Also, since the processor "rolls" from top to bottom of the data set along the direction of the tracks cyclic buffers could be used to perform the along track convolution prior to across track spline interpolation.

The sinc function design defined above was used for the along track filter. The problem is to adjust $f_c$ and N to most closely match the characteristics of the cubic spline thus producing an isotropic reconstruction. The along track filter was designed with the $f_c$=1/2D or the across track Nyquist frequency.

With $D \cong 30d$ in the problem at hand the filter is of the form:

$$h_x(k) = \frac{1}{D}\left\{\frac{\sin \pi k/30}{\pi k/30}\right\} \ (.5 + .5 \cos \pi k/N)$$

and the problem remains to choose N to cause the frequency response to match that of the cubic spline. Figure 8 contains $e_I$ as a function of the length N of the along track filter. The minimum anisotropic filter error is observed for N=105 and this is the optimum half length of the along track FIR filter.

The system structure for the filtering-interpolation algorithm is presented in Figure 9. The original survey data is stored with latitude and longitude for each sample in arbitrary locations on tape. A reformatting program not shown places each sample in its appropriate location in a 500 ft. planar grid precisely defined with reference to latitude and longitude. Unfilled cells are set to zero. This reformatted tape is then read by the reconstruction processor and the track locator searches across each data line and finds the data values for each track (NT=52 in this case) and places the data in the cyclic buffers. The FIR along track filter operations are performed and the current filtered line is available in the center position of each buffer. The filtered center values are sent to the spline parameter processor where the four coefficients for a cubic polynomial for each of the NT-1 intervals are computed. These coefficients go to the evaluator where N new values are generated between each track ($N \approx 30$). The full line is then written on the output tape and a new line of track samples is read in.

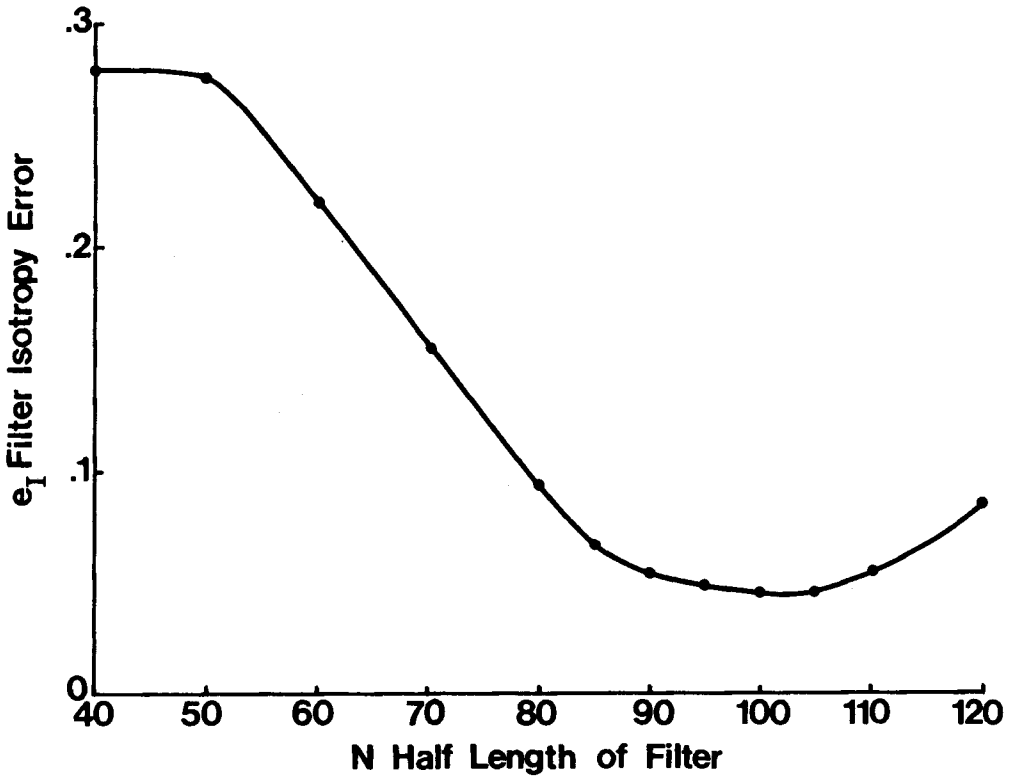


Figure 8. Isotropy Error $e_I$ as a Function of Half Length of the Along Track Filter.

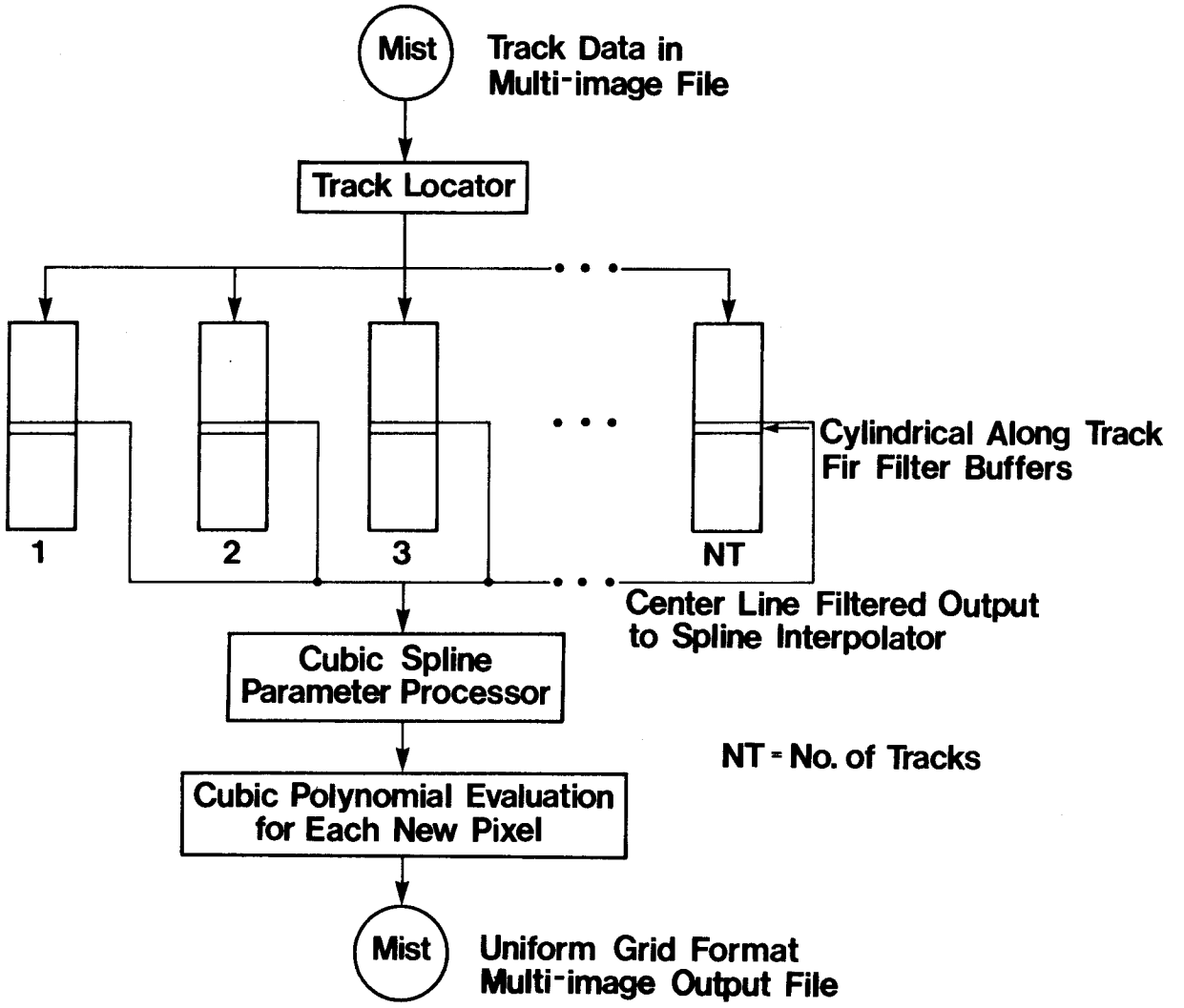


Figure 9. System Diagram for Cubic Spline/FIR Track-Type Data Reconstruction Algorithm.

For data structures such as this the mixed spline/FIR approach appears to be attractive. The coefficient generation process requires 4(M-2) multiplies or divides where M is the number of tracks. Evaluation of the cubic polynomials requires 3(M-1)N multiplies where N is the number of new points between each track. A four point FIR or cubic interpolating function would require a total of 4(M-1)·N multiplies. For the case here this is 4743 vs. 6120 respectively. Thus, a significant savings in processing is obtained plus the ease of implementation is improved. Figure 10 contains an isotropically reconstructed version of the data used for Figures 2 and 3. The shapes of features in this image are correct except for aliasing up to the bandwidth dictated by the across track sampling and should enable analysis with a minimum of confusion due to image reconstruction artifacts.

## VII. SUMMARY

Polynomial and sinc function based FIR interpolators were evaluated for use in isotropic reconstruction of track-type survey data. The cubic spline polynomial interpolator was shown to have superior frequency response characteristics compared to similar degree polynomial or FIR filter methods. A track-type data reconstruction algorithm was presented which uses the cubic spline for across track interpolation and FIR filter for along track frequency matching.

Several assumptions were made which simplified the problem but which appear to be reasonable. The track spacing was assumed to be constant and the along track samples were assumed uniformly

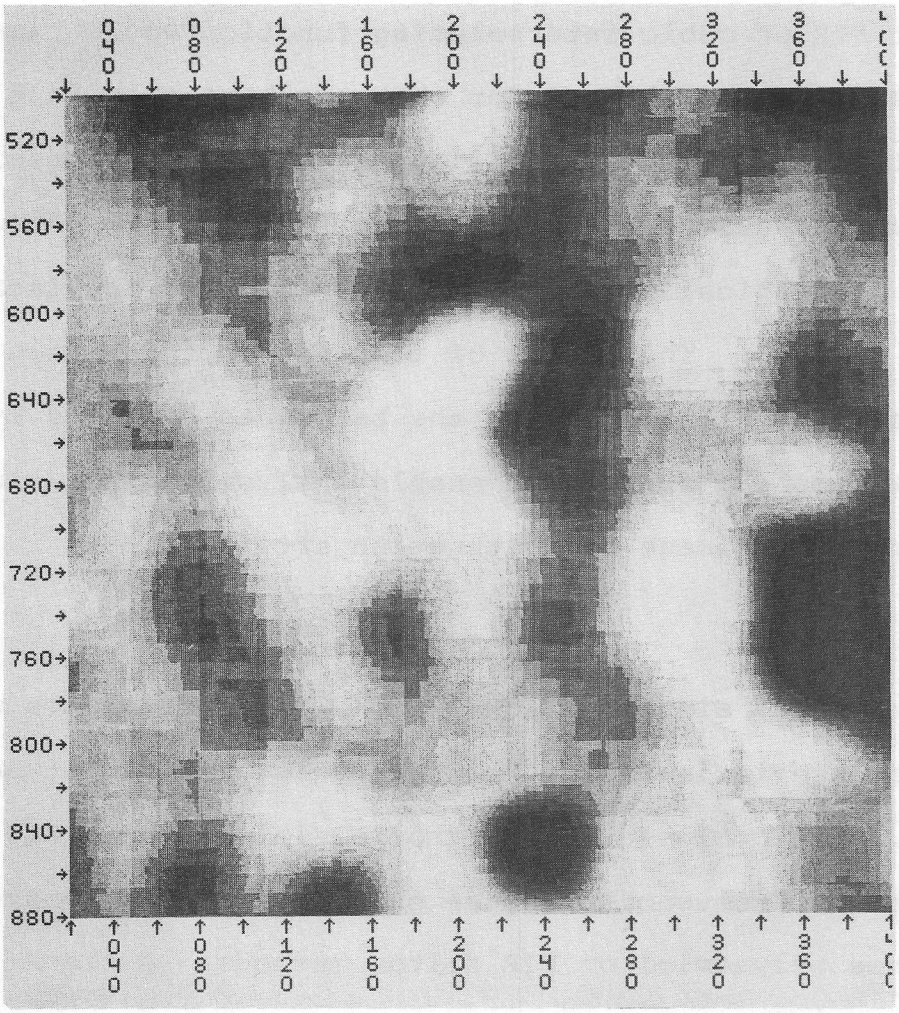


Figure 10. Isotropic Image Reconstruction of Uranium Gamma Ray Survey Data.

spaced. In actuality gaps exist in the data and the FIR filter smothes these intervals as if the data values were zero which is not a good approximation and this problem is left for future study. The SANR was introduced but not used since alias control was not implemented in the work reported here. The along track FIR filter had an optimum length of 105 and this is extremely costly and not recommended for implementation especially when cost is a prime consideration. If a 10% isotropy error is allowed the filter length can be reduced to N=75 which results in considerable savings. Further studies are needed to reduce along track computation costs to the order required for across track.

## VIII. REFERENCES

1. Cameron, G. W., Elliott, B. E., Richardson, K. A., "Effects of Line Spacing on Contoured Airborne Gamma-Ray Spectrometry Data," Proceedings of Symposium on Exploration for Uranium Ore Deposits, International Atomic Energy Agency, Vienna, Austria, March 29-April 2, 1976.

2. "Airborne Geophysical Survey-Southeast Arizona," Exploration Services Report GJO-1643, Texas Instruments Inc., Dallas, Texas, 1975.

3. Oppenheim, A. V., Schafer, R. W., "Digital Signal Processing," Prentice-Hall, Englewood Cliffs, N.J., 1975.

4. Rice, J. R., "Approximation of Functions," Vol. 2, Addison-Wesley Reading, Mass. 1964.

5. Schafer, R. W., Rabiner, L. R., "A Digital Signal Processing Approach to Interpolation," Proc. of IEEE Vol. 61, No. 6, June 1973, pp. 692-702.

6. Horowitz, H. L., "The Effects of Spline Interpolation on Power Spectral Density," IEEE Transactions on Acoustics, Speech and Signal Processing, Vol. ASSP-22, No. 1, Feb. 1974, pp. 22-27.

# APPENDIX

## POWER TRANSFER FUNCTIONS FOR INTERPOLATING METHODS

1. Linear Interpolation (same as 1st degree spline)

The interpolating pulse is a triangular function of width 2D:

$$h(x) = \left(1-\frac{|x|}{D}\right) \qquad -D \leq x \leq D$$

It is assumed in all the cases that the sample interval is D (meters, feet, etc.). The Fourier transform is then:

$$FT = \int_{-D}^{0} (1 + \frac{x}{D}) e^{-j\omega x} dx + \int_{0}^{D} (1 - x/D) e^{-j\omega x} dx$$

$$= \int_{-D}^{0} e^{-j\omega x} dx + \int_{-D}^{0} \frac{x}{D} e^{-j\omega x} dx + \int_{0}^{D} e^{-j\omega x} - \int_{0}^{D} \frac{x}{D} e^{-j\omega x} dx$$

$$= \frac{e^{-j\omega x}}{(-j\omega)} \int_{-D}^{0} + \frac{\frac{x}{D} e^{-j\omega x}}{(-j\omega)} \int_{-D}^{0} \frac{1/D e^{-j\omega x}}{(-j\omega)^2} \int_{-D}^{0}$$

$$+ \frac{e^{-j\omega x}}{(-j\omega)} \int_{0}^{D} - \frac{x/D e^{-j\omega x}}{(-j\omega)} \int_{0}^{D} + \frac{1/D e^{-j\omega x}}{(-j\omega)^2} \int_{0}^{D}$$

$$= \frac{1}{(-j\omega)} - \frac{e^{j\omega D}}{(-j\omega)} + \frac{e^{j\omega D}}{(-j\omega)} - \frac{1/D}{(-j\omega)^2} + \frac{1/D e^{j\omega D}}{(-j\omega)^2}$$

$$+ \frac{e^{-j\omega D}}{(-j\omega)} - \frac{1}{(-j\omega)} - \frac{e^{-j\omega D}}{(-j\omega)} + \frac{1/De^{-j\omega D}}{(-j\omega)^2} - \frac{1/D}{(-j\omega)^2}$$

$$= \frac{2/D}{\omega^2} - \frac{1/D}{\omega^2}(e^{-j\omega D} + e^{j\omega D}) = \frac{2}{D\omega^2}(1 - \cos\omega D)$$

$$= \frac{2}{D\omega^2}(2\sin^2\frac{\omega D}{2}) = D\left[\frac{\sin\frac{\omega D}{2}}{\frac{\omega D}{2}}\right]^2$$

The power transfer function is then:

$$|H_1(v)|^2 = D^2\left[\frac{\sin\pi ud}{\pi ud}\right]^4 \text{ for } u=\frac{\omega}{2\pi}$$

and normalizing so the transfer functions have unity magnitude at u=0 we have:

$$|H_1(v)|^2 = \left[\frac{\sin\pi uD}{\pi ud}\right]^4$$

## 2. Fourier Transform of Cubic Interpolation Pulse

The cubic interpolation pulse has a shape as diagrammed below and is expressed by four segment polynomials derived from the Lagrange equations:

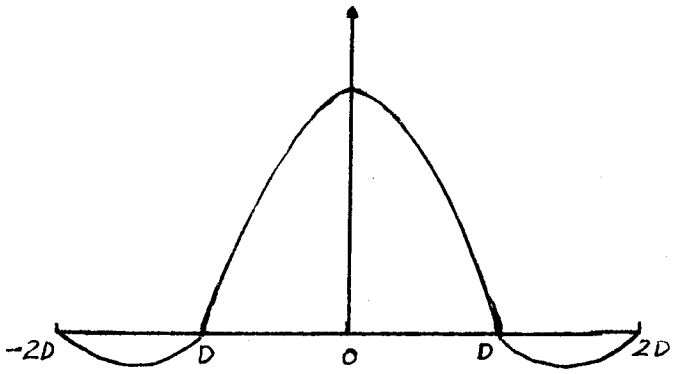


$$f(x) = \frac{1}{6}(3+x)(2+x)(1+x) \quad -2 \leq x \leq -1$$
$$f(x) = \frac{1}{2}(1+x)(1-x)(2+x) \quad -1 \leq x \leq 0$$
$$f(x) = \frac{1}{2}(x+1)(1-x)(2-x) \quad 0 \leq x \leq 1$$
$$f(x) = -\frac{1}{6}(x-1)(2-x)(3-x) \quad 1 \leq x \leq 2$$

These equations expand to:

$$f(x) = \frac{1}{6}(x^3 + 6x^2 + 11x + 6) \quad -2 \leq x \leq -1$$
$$f(x) = \frac{1}{2}(-x^3 - 2x^2 + x + 2) \quad -1 \leq x \leq 0$$
$$f(x) = \frac{1}{2}(x^3 - 2x^2 - x + 2) \quad 0 \leq x \leq 1$$
$$f(x) = -\frac{1}{6}(x^3 - 6x^2 + 11x - 6) \quad 1 \leq x \leq 2$$

The main lobe will be treated as one transform and the two sidelobes another to maintain symmetry. Note that the segments have discontinuous derivatives at -1, 0, and 1 making this a more complex transform than if only one function was involved. The Fourier transform of the main lobe is computed as follows:

$$FT_{MAIN} = \frac{1}{2}\left[-\int_{-1}^{0} x^3 e^{-j\omega x}dx - 2\int_{-1}^{0} x^2 e^{-j\omega x}dx + \int_{-1}^{0} x e^{-j\omega x}dx\right.$$

$$+ 2\int_{-1}^{0} e^{-j\omega x}dx + \int_{0}^{1} x^3 e^{-j\omega x} - 2\int_{0}^{1} x^2 e^{-j\omega x}dx$$

$$\left. - \int_{0}^{1} x e^{-j\omega x}dx + 2\int_{0}^{1} e^{-j\omega x}dx\right]$$

$$= \frac{1}{2}\left[-\left\{\frac{x^3\, e^{-j\omega x}}{(j\omega)} - \frac{3x^2\, e^{-j\omega x}}{(-j\omega)^2} + \frac{6x\, e^{-j\omega x}}{(-j\omega)^3} - \frac{6\, e^{-j\omega x}}{(-j\omega)^4}\right\}\right.$$

$$- 2\left\{\frac{x^2\, e^{-j\omega x}}{(-j\omega)} - \frac{2x\, e^{-j\omega x}}{(-j\omega)^2} + \frac{2\, e^{-j\omega x}}{(-j\omega)^3}\right\}$$

$$\left. + \left\{\frac{x\, e^{-j\omega x}}{(-j\omega)} - \frac{e^{-j\omega x}}{(-j\omega)^2}\right\} + \frac{2\, e^{-j\omega x}}{(-j\omega)}\right]_{-1}^{0}$$

$$+ \frac{1}{2}\left[\left\{\frac{x^3\, e^{-j\omega x}}{(-j\omega)} - \frac{3x^2\, e^{-j\omega x}}{(-j\omega)^2} + \frac{6x\, e^{-j\omega x}}{(-j\omega)^3} - \frac{6\, e^{-j\omega x}}{(-j\omega)^4}\right\}\right.$$

$$- 2\left\{\frac{x^2\, e^{-j\omega x}}{(-j\omega)} - \frac{2x\, e^{-j\omega x}}{(-j\omega)^2} + \frac{2\, e^{-j\omega x}}{(-j\omega)^3}\right\}$$

$$\left. - \left\{\frac{x\, e^{-j\omega x}}{(-j\omega)} - \frac{e^{-j\omega x}}{(-j\omega)^2}\right\} + \frac{2\, e^{-j\omega x}}{(-j\omega)}\right]_{0}^{1}$$

$$= \frac{1}{2}\left[\frac{6}{(-j\omega)^4} - \frac{4}{(-j\omega)^3} - \frac{1}{(-j\omega)^2} + \frac{2}{(-j\omega)} + \left(\frac{-1}{(-j\omega)} - \frac{3}{(-j\omega)^2}\right.\right.$$

$$\left.\frac{-6}{(-j\omega)^3} - \frac{6}{(-j\omega)^4}\right) e^{j\omega} + 2\left(\frac{1}{(-j\omega)} + \frac{2}{(-j\omega)^2} + \frac{2}{(-j\omega)^3}\right)e^{j\omega}$$

$$\left.- \left(\frac{-1}{(-j\omega)} - \frac{1}{(-j\omega)^2}\right)e^{j\omega} - \frac{2\,e^{j\omega}}{(-j\omega)}\right]$$

$$+ \frac{1}{2}\left[\left(\frac{1}{(-j\omega)} - \frac{3}{(-j\omega)^2} + \frac{6}{(-j\omega)^3} - \frac{6}{(-j\omega)^4}\right)\bar{e}^{j\omega} - 2\left(\frac{1}{(-j\omega)}\right.\right.$$

$$\left.- \frac{2}{(-j\omega)^2} + \frac{2}{(-j\omega)^3}\right)\bar{e}^{j\omega} - \left(\frac{1}{(-j\omega)} - \frac{1}{(-j\omega)^2}\right)\bar{e}^{j\omega} + \frac{2\,\bar{e}^{j\omega}}{(-j\omega)}$$

$$\left.+ \frac{6}{(-j\omega)^4} + \frac{4}{(-j\omega)^3} - \frac{1}{(-j\omega)^2} - \frac{2}{(-j\omega)}\right]$$

$$= \frac{1}{2}\left[\frac{12}{\omega^4} + \frac{2}{\omega^2} + \frac{(-1+2+1-2)}{(-j\omega)}\,(e^{j\omega} - \bar{e}^{j\omega}) + \frac{-6+4}{(-j\omega)^3}\,(e^{j\omega} - \bar{e}^{j\omega})\right.$$

$$\left.+ \frac{(-3+4+1)}{(-j\omega)^2}\,(e^{j\omega} + \bar{e}^{j\omega}) + \frac{-6}{(-j\omega)^4}\,(e^{j\omega} + \bar{e}^{j\omega})\right]$$

$$= \frac{6}{\omega^4} - \frac{3}{\omega^4}\,2\,\cos\omega + \frac{1}{\omega^2} - \frac{1}{j\omega^3}\,2j\,\sin\omega - \frac{1}{\omega^2}\,2\,\cos\omega$$

$$= \frac{6}{\omega^4}\,2\,\sin^2\omega/2 - \frac{2}{\omega^3}\,\sin\omega + \frac{1}{\omega^2} - \frac{2}{\omega^2}\,\cos\omega$$

$$= \frac{6}{\omega^4}\, 2\, \sin^2\omega/2 + \frac{2\, \sin^2\omega/2}{\omega^2} - \frac{2}{\omega^3}\, \sin\omega - \frac{\cos\omega}{\omega^2}$$

$$FT_{SIDE} = \frac{1}{6}\left[\int_{-2}^{-1} x^3 e^{-j\omega x}dx + 6\int_{-2}^{-1} x^2 e^{-j\omega x}dx + 11\int_{-2}^{-1} x\, e^{-j\omega x}\right.$$

$$+ 6\int_{-2}^{-1} e^{-j\omega x}dx - \int_{+1}^{2} x^3 e^{-j\omega x}dx + 6\int_{1}^{2} x^2 e^{-j\omega x}dx$$

$$\left. - 11\int_{1}^{2} x\, e^{-j\omega x}dx + 6\int_{1}^{2} e^{-j\omega x}dx\right]$$

$$= \frac{1}{6}\left[\left(\frac{x^3}{(-j\omega)} - \frac{3x^2}{(-j\omega)^2} + \frac{6x}{(-j\omega)^3} - \frac{6}{(-j\omega)^4}\right)e^{-j\omega x} + 6\left(\frac{x^2}{(-j\omega)} - \frac{2x}{(-j\omega)^2}\right.\right.$$

$$\left.\left. + \frac{2}{(-j\omega)^3}\right)e^{-j\omega x} + 11\left(\frac{x}{(-j\omega)} - \frac{1}{(-j\omega)^2}\right)e^{-j\omega x} + \frac{6\, e^{-j\omega x}}{(-j\omega)}\right]_{-2}^{-1}$$

$$+ \frac{1}{6}\left[-\left(\frac{x^3}{(-j\omega)} - \frac{3x^2}{(-j\omega)^2} + \frac{6x}{(-j\omega)^3} - \frac{6}{(-j\omega)^4}\right)e^{-j\omega x} + 6\left(\frac{x^2}{(-j\omega)} - \frac{2x}{(-j\omega)^2}\right.\right.$$

$$\left.\left. + \frac{2}{(-j\omega)^3}\right)e^{-j\omega x} - 11\left(\frac{x}{(-j\omega)} - \frac{1}{(-j\omega)^2}\right)e^{-j\omega x} + \frac{6\, e^{-j\omega x}}{(-j\omega)}\right]_{1}^{2}$$

$$= \frac{1}{6}\left[\left(\frac{-1}{(-j\omega)} - \frac{3}{(-j\omega)^2} - \frac{6}{(-j\omega)^3} - \frac{6}{(-j\omega)^4}\right)e^{j\omega} + 6\left(\frac{1}{(-j\omega)} + \frac{2}{(-j\omega)^2}\right.\right.$$

$$\left.\left. + \frac{2}{(-j\omega)^3}\right)e^{j\omega} + 11\left(\frac{-1}{(-j\omega)} - \frac{1}{(-j\omega)^2}\right)e^{j\omega} + \frac{6\, e^{j\omega}}{(-j\omega)}\right.$$

$$- \left( \frac{-8}{(-j\omega)} - \frac{12}{(-j\omega)^2} - \frac{12}{(-j\omega)^3} - \frac{6}{(-j\omega)^4} \right) e^{j2\omega} - 6 \left( \frac{4}{(-j\omega)} + \frac{4}{(-j\omega)^2} \right.$$

$$\left. + \frac{2}{(-j\omega)^3} \right) e^{j2\omega} - 11 \left( \frac{-2}{(-j\omega)} - \frac{1}{(-j\omega)^2} \right) e^{j2\omega} - \frac{6\, e^{j2\omega}}{(-j\omega)}$$

$$- \left( \frac{8}{(-j\omega)} - \frac{12}{(-j\omega)^2} + \frac{12}{(-j\omega)^3} - \frac{6}{(-j\omega)^4} \right) \bar{e}^{2\omega j}$$

$$+ 6 \left( \frac{4}{(-j\omega)} - \frac{4}{(-j\omega)^2} + \frac{2}{(-j\omega)^3} \right) \bar{e}^{j2\omega} - 11 \left( \frac{2}{(-j\omega)} - \frac{1}{(-j\omega)^2} \right) \bar{e}^{j2\omega}$$

$$+ \frac{6}{(-j\omega)^4} e^{j2\omega} + \left( \frac{1}{(-j\omega)} - \frac{3}{(-j\omega)^2} + \frac{6}{(-j\omega)^3} - \frac{6}{(-j\omega)^4} \right) \bar{e}^{j\omega}$$

$$- 6 \left( \frac{1}{(-j\omega)} - \frac{2}{(-j\omega)^2} + \frac{2}{(-j\omega)^3} \right) \bar{e}^{j\omega} + 11 \left( \frac{1}{(-j\omega)} - \frac{1}{(-j\omega)^2} \right) \bar{e}^{j\omega}$$

$$\left. - \frac{6\, \bar{e}^{j\omega}}{(-j\omega)} \right]$$

$$= \frac{1}{6} \left[ \frac{-1+6-11+6}{(-j\omega)} (e^{j\omega} - \bar{e}^{j\omega}) + \frac{-3+12-11}{(-j\omega)^2} (e^{j\omega} + \bar{e}^{j\omega}) \right.$$

$$+ \frac{-6+12}{(-j\omega)^3} (e^{j\omega} - \bar{e}^{j\omega}) - \frac{6}{(-j\omega)^4} (e^{j\omega} + \bar{e}^{j\omega})$$

$$+ \frac{8-24+22-6}{(-j\omega)} (e^{j\omega 2} - \bar{e}^{j\omega 2}) + \frac{12-24+11}{(-j\omega)^2} (e^{j2\omega} + \bar{e}^{j2\omega})$$

$$+ \frac{12 - 12}{(-j\omega)^3} (e^{j2\omega} - e^{-j2\omega}) + \frac{6}{(-j\omega)^4} (e^{j2\omega} + e^{-j2\omega}) \Bigg]$$

$$= \frac{1}{6} \Bigg[ + \frac{2}{\omega^2} \; 2\cos\omega + \frac{6}{j\omega^3} 2j \sin\omega - \frac{6}{\omega^4} 2\cos\omega$$

$$+ \frac{1}{\omega^2} 2\cos 2\omega + \frac{6}{\omega^4} 2\cos 2\omega \Bigg]$$

$$= \frac{2/3\cos\omega + 1/3\cos 2\omega}{\omega^2} - \frac{2(\cos\omega - \cos 2\omega)}{\omega^4} + \frac{2\sin\omega}{\omega^3}$$

$$\text{Total Transform} = \frac{12}{\omega^4} \sin\omega/2 - \frac{2}{\omega^3} \sin\omega + \frac{2}{\omega^2} \sin\omega/2 - \frac{\cos\omega}{\omega^2}$$

$$- \frac{2(\cos\omega - \cos 2\omega)}{\omega^4} + \frac{2\sin\omega}{\omega^3} + \frac{2/3\cos\omega + 1/3\cos 2\omega}{\omega^2}$$

$$= \frac{12}{\omega^4} \sin^2(\omega/2) + \frac{2(1 - 2\sin^2\omega)}{\omega^4} - \frac{2\cos\omega}{\omega^4} + \frac{2\sin^2(\omega/2)}{\omega^2}$$

$$+ \frac{1/3(1 - 2\sin^2\omega)}{\omega^2} + \frac{2/3\cos\omega}{\omega^2} - \frac{\cos\omega}{\omega^2}$$

$$= \frac{12}{\omega^4} \sin^2(\omega/2) - \frac{4\sin^2\omega}{\omega^4} + \frac{4\sin^2\omega/2}{\omega^4} + \frac{2\sin^2(\omega/2)}{\omega^2}$$

$$- \frac{2/3\sin^2\omega}{\omega^2} + \frac{2/3\sin^2(\omega/2)}{\omega^2}$$

$$= \frac{16}{\omega^4}\sin^2(\omega/2) - \frac{4\sin^2\omega}{\omega^4} - \frac{2/3\sin^2\omega}{\omega^2} + \frac{8/3\sin^2(\omega/2)}{\omega^2}$$

$$= \frac{\sin^2(\omega/2)}{(\omega/2)^4} - \frac{4\sin^2\omega}{\omega^4} - \frac{2}{3}\frac{\sin^2\omega}{\omega^2} + \frac{8}{12}\frac{\sin^2(\omega/2)}{(\omega/2)^2}$$

The square of this function for $\omega=2\pi u$ is evaluated and used in Figures 6 and 7.

3. Transform for Fifth Degree Polynomial Interpolation

Transforms of higher degree are clearly extremely cumbersome and numerical methods must be used. For the fifth degree polynomial interpolator the Lagrange interpolating pulse values were determined and Fourier transformed to obtain the frequency response. The samples of the interpolating pulse for five new points to be generated between each original data pair are given by (5):

$$h(i) = \frac{-1}{12}(.2i+2)(.2i+1)(.2i-1)(.2i-2)(.2i-3) \qquad i=0,\ldots,4$$

$$h(i) = \frac{1}{24}(.2i+2)(.2i)(.2i-1)(.2i-2)(.2i-3) \qquad i=5,\ldots,9$$

$$h(i) = \frac{-1}{120}(.2i+1)(.2i)(.2i-1)(.2i-2)(.2i-3) \qquad i=10,\ldots,14$$

$$h(-i) = h(i)$$

These values were Fourier transformed and the magnitude squared plotted in Figures 6 and 7.

4. Power Transfer Functions of Spline Interpolators

The spline polynomials are specified by data and continuity conditions at each of the joints between polynomials. A derivation

by Horowitz (6) starts with a piecewise linear expression for the Q-kth derivative for a Q degree spline and integrates this expression Q-1 times to get an expression for the polynomial values in terms of Q-1 constants for each interval. Applying value and derivative continuity conditions at all interior joints a system of QR + 2 - Q equations is generated (where R is the number of intervals) which yield a difference equation for the Q-1th derivative at each joint (data point) in terms of the data value at each point. For the cubic and fifth degree splines these are:

$$\text{Cubic:} \quad \frac{1}{6}\,(y_{k+1} + 4y_k + y_{k-1}) = (x_{k+1} - 2x_k + x_{k-1})\,\frac{1}{D^2}$$

$$\text{Fifth:} \quad \frac{1}{120}\,(y_{k+1} + 26y_k + 66y_{k-1} + 26y_{k-2} + y_{k-3}) = (x_{k+1} - 4x_k + 6x_{k-1} - 4x_{k-2} + x_{k-3})\,\frac{1}{D^4}$$

where: $x_k$ is the data value at the kth joint

$y_k$ is the Q-1th derivative at the kth point. (Q=3 and 5 respectively.)*

The Z transform of these expression are then computed:

$$H_3(z) = \left(\frac{z-2+z^{-1}}{z+4+z^{-1}}\right)\left(\frac{6}{D^2}\right)$$

---

* Departure from the previous convention where x and y are independent variables is made here to maintain the notation of Horowitz.

$$H_5(z) = \left(\frac{z-4+6z^{-1}-4z^{-2}+z^{-3}}{z+26+66z^{-1}+26z^{-2}+z^{-3}}\right)\left(\frac{120}{D^4}\right)$$

These relate the Q-1 derivative to the input data $H(z) = \frac{Y(z)}{X(Z)}$

The Fourier transform of the sampled sequence is expressed:

$$X^*(v) = \frac{1}{D}\sum_{k=-\infty}^{\infty} X(v-k/D)$$

Where: X is the FT of the input.

The z transforms are then converted to functions of frequency:

$$H_3(e^{j2\pi vD}) = \frac{(\cos 2\pi vD-1)}{(2+\cos 2\pi vD)}\left(\frac{6}{D^2}\right)$$

$$H_5(e^{j2\pi vD}) = \frac{(6-8\cos 2\pi vD+2\cos 4\pi vD)}{(66+52\cos 2\pi vD+2\cos 4\pi vD)}\frac{120}{D^2}$$

The Fourier transform of the sequence of Q-1th derivative samples is then available as:

$$Y(e^{j2\pi vD}) = X(e^{j2\pi vD})\ H(e^{j2\pi vD})$$

The spline interpolated signal is obtained by linearly interpolating the Q-1th derivative samples and integrating Q-1 times. This results in:

$$F(p(t)) = \left(\frac{1}{j2\pi v}\right)^{\Omega-1} \left(\frac{\sin\pi vD}{\pi vD}\right)^{2} H(e^{j2\pi vD}) \sum_{k=-\infty}^{\infty} X(v-k/D)$$

where: p(t) is the spline reconstructed signal with t being used as the independent variable as taken from Horowitz.

This development is valid for an infinite sequence of spline intervals and the derministic signal case. The power transfer function for this case would be the magnitude squared of the terms not depending on X in the above expression which for the two cases at hand are:

$$|H_3(v)|^2 = \left(\frac{3}{2+\cos 2\pi vD}\right)^2 \left(\frac{\sin\pi vD}{\pi vD}\right)^8$$

$$\left|H_5(v)\right|^2 = \frac{(120)^2}{(2\pi vD)^8} \left(\frac{6-8\cos 2\pi vD+2\cos 4\pi vD}{66+52\cos 2\pi vD+2\cos 4\pi vD}\right)^2 \left(\frac{\sin\pi vD}{\pi vD}\right)^4$$

Thus the transfer function for the infinite data set appears to be valid without making the further assumption that the input is a white random process. The substitution is made by Horowitz that:

$$X(v) = S_{xx}(v)$$

$$S_{xx}(v) = D|X_D(v)|^2$$

and

$$X_D(v) = \frac{1}{D} \int_{-D/2}^{D/2} x(t)\ e^{-j2\pi vt} dt$$

in the limit as $D \longrightarrow \infty$. A white bandlimited input process is assumed with bandwidth limited to 1/2D which produces a constant sampled spectrum: $S_{xx}(v) = 1$, $\infty \leq v \leq \infty$. The result for purposes of comparison of interpolators is the same as assuming X is deterministic and using the $|H(v)|^2$ as derived above. The spectral density assumption; however, appears to be incorrect. The transform $X_D(v)$ does not converge to the power spectrum as shown in Davenport and Root. The correct approach is to use an ensemble expectation to get the nonstationary power spectral density then take a time average to get the time independent density.

The question which remains is the effect of finite data sets on the spline transfer function results. This is left for further study.